Comparative study of the adsorption of SO_4^{2-}/HSO_4^- and Cl^- anions on smooth and rough surfaces of noble metal electrodes by in-situ radiotracer thin gap method

Kata Berkesi[*1], Dávid Horváth, Zoltán Németh, Kálmán Varga[†]
University of Pannonia, Institute of Radiochemistry and Radioecology, H-8200 Veszprém, Egyetem street 10, Hungary

László Péter
Wigner Research Centre for Physics, Hungarian Academy of Sciences H-1525 Budapest, P.O. Box: 49., Hungary

Tamás Pintér
Paks Nuclear Power Plant Ltd., H-7031 Paks, PO. Box: 71., Hungary

Abstract

The so-called in-situ thin gap method for the measurement of the surface excess of the radiolabelled species was originally designed for the application of noble metal electrodes with low surface roughness. Therefore, the observation of adsorbed species containing radioisotopes of high specific activity (i.e., ^{35}S and ^{14}C) was only possible. A recent extension of the original thin gap method to metals with a surface roughness factor higher than 10, however, made it possible to follow the adsorption of species with low specific activity (i.e., ^{36}Cl). Based on the validation of the improved thin gap method *[Horváth et al, Electrochim. Acta 109 (2013) 468],* this study aims at the comparison of the sulfate/bisulfate and chloride adsorption on both smooth (Pt and Au) and rough (platinized platinum) noble metal electrodes. It was found that the radiation signal of the adsorbed chloride ions can also be detected, and the surface excess of both radiolabelled bisulfate and chloride ions can be measured. The accumulation of the adsorbed species on rough electrodes took place at a much longer time scale than the removal of the same species. No such difference was found for smooth electrodes. The apparent asymmetry in the temporal behaviour of the adsorption and desorption processes on rough electrodes could be understood by the difference in the concentration gradient in the solution near or within the porous structures during the respective processes.

Keywords: in-situ thin gap method, sulfate/bisulfate and chloride anion adsorption, smooth and rough noble metal surfaces, relative adsorption strength

[*] Corresponding author. E-mail: berkesi.kata@wigner.mta.hu, Tel: +36 1 392 2222 Fax: +36 1 392 2768
[1] Present adress: Wigner Research Centre for Physics, Hungarian Academy of Sciences, H-1525 Budapest, P.O. Box: 49., Hungary
[†] The authors wish to dedicate this paper to the belowed memory of Prof. K. Varga who deceased during the course of the present work in February 2012.

1. Introduction

The in-situ radiotracer methods play a crucial role in the study of adsorption/desorption phenomena on liquid/solid interfaces. The principle of radioisotope indication was originally suggested by György Hevesy (1913) [1,2]. In 1930 F. Joliot-Curie [3] was the first who applied this method to investigate the interfaces of solid/liquid systems, specifically to study the electrochemical separation of polonium. The principal idea of the so-called in-situ radiotracer "foil" method comes from this experiment. In the 1950s, a significant development of the radiotracer technique began, and tools of several research groups were flared by these methods. However, these in-situ radiotracer methods for electrosorption research are used nowadays in less than 10 laboratories worldwide, as summarized in the work of Horányi [4].

The in-situ radiotracer technique includes the following main advantages [5]:

- it is nuclide specific;
- it gives a direct and in-situ information about the mass transfer processes from/towards the interface;
- it is extraordinarily sensitive, detection limit: $1 > \Theta \geq 2*10^{-6}$ monolayer (ML);
- the radioisotope labelling of the compound to be used as the adsorbate can be easily performed;
- by choosing an appropriate method, the material of the surface tested and the crystallographic orientation can be selected.

Besides the advantageous properties of the methods, they have some inherent features that impose certain limitations to the information to be gained:

- the adsorption mode (geometry) of a species remains hidden (i.e., it cannot be established which atom of the adsorbed species is direcly bonded to the surface);
- the crystallographic orientation of the substrate cannot be arbitrary chosen and no sigle-crystal conditions can be applied (i.e., in the case of the foil method).

The radiotracer methods used for the examination of adsorption/desorption constitute an advanced group of in-situ surface tests by which the surface excess (radioactivity) of the adsorbeate can be continuously measured on the surface of the electrode. All of the relevant procedures are based on the so-called "thin-layer" principle developed by Aniansson [6]. The

concept of the thin-layer principle is that the total radioactivity of the entire solid/liquid interface is determined (where the "interface" includes here the surface tested and a limited volume of the contact solution). This method is viable in the case when the radiolabelled isotopes emit β^--particles with low- or medium-energy and γ(X-ray)- photons of energy below 20 keV. If the radioactively labelled species enrich on the studied surface, they are added to the detector sight. The radiation intensity increment measured is proportional to the entered quantity. The most often applied pure β –emitting radioisotopes in these measurements are ^{3}H [7, 8], ^{14}C [9-12], ^{32}P [13, 14], ^{35}S [4, 5, 13, 15-25] and ^{36}Cl [13, 16, 22, 25-32].

The so-called “electrode-lowering” method is based on the thin-layer principle. This technique was developed in the late of the 1960s by Kazarinov et al. The method was further developed in the early 1970s and it was referred to later as the “thin gap” method [33]. In the cell developed for the thin gap method, the intensity of the adsorption process can be measured alternately in two different positions of the working electrode: (i) pressed to the membrane forming the bottom of the cell (the background radiation can be minimized); and (ii) removed to a large distance from the bottom wall of the cell (in the case of using β^--emitting isotopes, the distance exceeds the escape depth of the radiation from the solution). According to the opinion of the inventors [6, 33], it is applicable to examine the adsorption characteristics of surfaces with small (γ<2) and high (γ>10) roughness factor in the case of using both β^-- and γ-emitting isotopes.

However, the original thin gap method was elaborated to study the adsorption on smooth surfaces. This fact implies that there were some strong limitations of the applicability of the original method considering both labelled species and metallic constructional materials to be investigated [34, 35]. For instance, the thin gap version of the above procedure did not allow to measure the adsorption/desorption processes and to determine quantitatively the surface excess (Γ) values of labelled species having low specific activity (chloride labelled with ^{36}Cl) on smooth surfaces (roughness factor<2). By a further development of the original methodology of the thin gap technique for the investigation of porous metal electrodes (roughness factor > 10), the sensitivity was increased and the detection limit was improved. As a fundamental demand in this regard, the expressions used for quantitative evaluation of Γ values on smooth surfaces were refined in some aspects (i.e. applicability for porous surfaces and for radionuclides having low specific activity). Following a methodological improvement,

we can get some information on the adsorption of radiolabelled species with low specific activity (^{36}Cl) on rough surfaces [36, 37].

The present work is focused on the comprehensive investigation of the applicability (advantages and limitations) of the original thin gap method for the study of the competitive sulfate/bisulfate (labelled with ^{35}S) and chloride (labelled with ^{36}Cl) adsorption on smooth Au and Pt electrodes in supporting electrolyte consisting of 0.1 mol dm^{-3} $HClO_4$. In addition, we report some new findings obtained upon the above adsorption processes in perchlorate solution containing H_3BO_3. Furthermore, we have investigated the adsorption of the aforementioned labelled anions on rough surfaces. A comparative study will be presented on the adsorption phenomena on two different surfaces including both labelled species.

2. Experimental

A combined radio-electrochemical cell – developed by Varga and coworkers [34, 36, 38, 39] – was applied for the adsorption experiments using in-situ thing gap method. The calculation of the surface excess values of sulfate/bisulfate and chloride ions took place on the basis of the intensity measurment of the emitted β^--radiation of ^{35}S ($E_{\beta max}$ = 167 keV) and ^{36}Cl ($E_{\beta max}$ = 714 keV) radionuclides used for labelling. By following the technical solution introduced in the 1970's [7, 8, 10, 11], electrons were detected by using a Li-glass scintillator (thickness: 5 mm) and an ORTEC® DSPEC LF™ type 8k multichannel analyzer (Ametek Inc., U.S.A.) was used to display the spectrum of the radiation. The light coupling between the scintillator and the 16-dinodes photoelectron multiplayer was ensured by an optical unit, and the necessary stable high voltage to the detector was produced by a Thorn- EMI PM28B type high-voltage power supply. Surface excess values of the adsorbed sulfate/bisulfate and chloride ions on smooth noble metal electrodes were accounted according to a calculation procedure outlined by Kolics [15]:

$$\Gamma = \frac{I_{ads}}{I_{gap}} \frac{cx}{\gamma} \tag{1}$$

The surface excess values of the adsorbed sulfate/bisulfate and chloride ions on rough surface of platinum black were calculated according to the equation outlined by Horváth and coworkers [36]:

$$\Gamma = \frac{I_{ads}}{I_{por} + I_{gap}} \cdot \frac{c}{\gamma} \cdot (\varepsilon k + d), \tag{2}$$

where the meaning of the symbols is as follows, Γ: surface excess [mol cm^{-2}], I_{ads}: intensity emitted by the adsorbed species [cpm], I_{gap}: intensity originating from the gap solution layer between the lowered electrode and the detector surface [cpm], I_{por}: intensity originating from the solution trapped in the porous layer [cpm], c: the chemical concentration of the labelled species in the solution [mol cm^{-3}], γ: roughness factor [dimensionless] that characterizes the real surface area exposed to the solution divided by the geometric surface area, ε: the porosity [dimensionless] describing the volume ratio of solution-filled pores in the surface layer and the total geometric volume of the surface layer, k: the thickness of the porous layer [cm], d: thickness of the gap [cm]. When the electrode is in the lowered position and polarized to achieve the complete desorption of the radiolabelled anions, the sum of $I_{gap} + I_{por}$ can be measured. In the case of the working electrode polarization to a potential where anion adsorption is possible, the measured intensity can be expressed as $I_{ads} + I_{gap} + I_{por}$.

Electrochemical measurements were carried out by an EF435 type potentiostat (Electroflex, Hungary) and voltammetric curves were registered by an XY Register (Upgrade Bt., Hungary). All measurements were conducted at room temperature (~22 °C). In this work, potential values are given on the reference hydrogen electrode scale (RHE); i.e. the potential values are referred to the reversible hydrogen electrode in the same solution (purity of H_2: 99.5 %, Messer Hungary). The reference electrode compartment was separated from the main chamber with a glass frit. Platinum wire was used as auxiliary electrode. Ar gas (purity: 99.999 % , Messer Hungary) was continuously bubbled through the solutions to eliminate the effects of O_2 and CO_2.

The smooth polycrystalline Pt(poly) and Au(poly) working electrodes, 10 mm in diameter and 3 mm height, 99.99 % in purity were acquired from Mateck GmbH (Germany). The real surface area of the Pt(poly) was determined in the 0.1 M $HClO_4$ solution from the charge required for the H adsorption in the cyclic voltammograms measured. The negative integration limit was the minimum of the cathodic current occurring before hydrogen evolution, assuming that one monolayer coverage with H-species consumes 210 μC cm^{-2} [16]. The surface roughness of polycrystalline platinum was found to be 1.2 to 1.3. The platinum black layer was produced as it is described in Ref: [37, 40-42]. The real surface area of the platinized platinum was determined with the same method as discussed above for the smooth Pt electrodes. The surface roughness of platinum black fell to the range of 12 to 69 [37]. The roughness factor increased with the thickness of the platinum layer deposited.

The real surface area of the Au(poly) was determined in the 0.1 M $HClO_4$ solution from the charge measured for surface oxidation by voltammetry, up to the current minimum occurring before oxygen evolution, assuming that one monolayer coverage with O-species corresponds to 400 μC cm^{-2} [15, 16]. The surface roughness of polycrystalline gold ranged from 1.1 to 1.4.

Highly purified water (Millipore Simplicity) and $HClO_4$ (Merck, Suprapur) was applied for the preparation of the solutions. In the adsorption experiments, the radiolabelled $H_2{}^{35}SO_4$ (Isotope Institute Gmbh., Hungary, molar activity: 3.7×10^{12} Bq mol^{-1}), $Na_2{}^{35}SO_4$ (ARC Inc., U.S.A., molar activity: 4×10^{12} Bq mol^{-1}) and $H^{36}Cl$ (ARC Inc., U.S.A., molar activity: 1×10^{10} Bq mol^{-1}) were used in a solution of 2×10^{-4} mol dm^{-3} concentration.

Before adsorption experiments, the polycrystalline electrodes were cyclically polarized in 0.1 mol dm^{-3} $HClO_4$ supporting electrolyte (sweep rate: 25 mV s^{-1}) in the potential range of 0.05 – 1.45 V and 0.06 – 1.65 V in the case of Pt(poly) and Au(poly) electrodes, respectively. In case of platinized platinum surface, the potential range of the cyclic voltammetric study fell in a range of 0.05 – 0.8 V to avoid the formation of chloride complexes with the platinum, wich could change the adsorption properties of the porous surface [39, 43-47]. The cyclic polarization pre-treatment was performed until stabilized voltammograms were measured. Subsequently, labelled anions were administered in the solution and a stabilized voltammetric curve was registered again.

The potential dependence of the sulfate/bisulfate and chloride adsorption on smooth noble metal surfaces was studied by the so-called “interrupted” polarization method [22]. In this procedure, several voltammetric scans (3-5) at a sweep rate of 100 mV s^{-1} were applied, ranging to the entire potential interval to be studied during the adsorption experiment. The scans performed with the above described pre-treatment renewed the electrode surface and removed the trace impurities. During the last scan, the actual measurement potential was approached from the negative potential limit; i.e, from the uncovered electrode state. A 10 s long saturation period was sufficient to achieve the equilibrium surface coverage and provided reproducible measurement conditions [17].

The determination of the potential dependence of the sulfate/bisulfate and chloride anion adsorption on rough surface of platinized platinum was studied by the continuous polarization mode. The electrode potential value was changed continuously without renewing the electrode surface by using potential scans [22].

3. Results and discussion

3.1. Results on smooth Pt(poly)

The adsorption of sulfate/bisulfate and chloride ions on Pt(poly) electrode surface with small roughness factor ($\gamma<2$) by using radiotracer methods is a well-known and widely studied phenomenon [4, 5, 15, 16, 18]. In this section, the most important results of some anion (HSO_4^-/SO_4^{2-}, Cl^-) adsorption on smooth electrode surface will be shown that highlights the advantages and limitations of the applicability of the original version of thin gap method. From cyclic voltammograms of the polycrystalline platinum it can be clearly seen that the added labelled anions affect the electrochemical behaviour of the surface. The possible causes of the different electrochemical behaviour of the solution including the labelled species will be explained below.

3.1.1. Adsorption of labelled SO_4^{2-}/HSO_4^- ions

Sulfate/bisulfate adsorption on smooth Pt(poly) is an often investigated phenomenon. In this section, the conformity of our system with the previously published literature data will be shown. In addition, the mobility of the sulfate/bisulfate anions in the presence on dissimilar ions (unlabelled HCl, H_3BO_3) was studied in order to assess the adsorption strength sequence of the anions studied.

The time dependence of sulfate/bisulfate adsorption is shown in Figure 1 at potential values of E = 750 mV and E = 1150 mV. The fast adsorption process of HSO_4^-/SO_4^{2-} is clearly demonstrated in Figure 1. The saturation surface excess at both potential values applied is achieved within a period of less than 10 seconds. The decrease of the surface excess at E = 750 mV potential value is caused by the trace amount of some contaminant ions present in the solution. The most likely sort of impurity is the chloride ion that is often present in perchloric acid solutions as the decomposition product of the perchlorate anion.

The cyclic voltammetric curves of polycrystalline platinum electrode measured in 0.1 mol dm^{-3} $HClO_4$ change when H_2SO_4 is also present (see Figure 2.a). These voltammograms are in good agreement with literature data [16, 17], which fact also indicates that the purity of platinum/$HClO_4$ system meets the electrochemical requirement. In the presence of sulfuric acid, the onset potential of the electro-oxidation of the platinum surface is shifted towards

positive values. This is caused by blocking of the active centres of the surface by adsorbed anions.

The surface excess values of HSO_4^-/SO_4^{2-} ions on polycrystalline platinum as a function of the electrode potential are shown in Figure 2.b. The functions obtained correspond well, within the experimental error, to the results published in the literature [17, 18]. The hysteresis observed between the anodic-going and cathodic-going polarization directions (i.e, curves 1 and 2) in Figure 2.b correlates with the potential difference of the electrooxidation and electroreduction of the polycrystalline platinum surface. The hysteresis in the surface excess function is a consequence of the difference in the steady-state oxide coverage as a function of the polarization direction.

The results of the mobility study of HSO_4^-/SO_4^{2-} ions are shown in Figures 3 through 5. As it can be seen, the adsorbed HSO_4^-/SO_4^{2-} ions can be mobilized from the surface but the effective foreign ion concentration necessary for the sulfate/bisulfate mobilization strongly depends on the nature of the unlabelled compound added. In the presence of unlabelled sulfuric acid (Fig. 3), the change in the surface concentration of the radiolabelled ions is proportional to the ratio of the concentration of labelled species to the overall sulfuric acid concentration. This indicates that the dissolved and adsorbed species are in a dynamic equilibrium. The time needed to achieve the equilibrium upon the addition of unlabelled sulfuric acid is only a few seconds.

When unlabelled boric acid is added to the Pt(poly)/bisulfate equilibrium system (see Fig. 4), the adsorbed sulfate/bisulfate ions can be partly expelled from the surface. For a significant adsorbate exchange effect, boric acid must be present in a much larger concentration than sulfuric acid. No bisulfate desorption can be established from the radiation intensity when boric acid is present in a five times larger concentration than the sulfuric acid labelled with ^{35}S. When the concentration ratio is increased to 50, approximately half of the bisulfate ions are forced to desorbe from the surface. Comparing to the equilibration times, one can see that the addition of boric acid causes a much slower bisulfate desorption than sulfuric acid, and the steady-state is difficult to achieve. The change of the bisulfate surface excess a few tens of seconds after the boric acid addition indicates that the active surface sites are not necessarily the same, the regularity of the adsorbate surface pattern may be much smaller when these two kinds of species are present or a mixed surface layer is generated.

As it can be seen from Figure 5, the impact of the chloride ions on the surface coverage of Pt with bisulfate ions is rather drastic – as it is clearly demonstrated in literature [19] – as compared to the impact of the boric acid. Even in a two orders of magnitude smaller

concentration than sulfuric acid the removal of the sulfate species from the Pt surface is significant (about 20%). When the chloride ion concentration is 20 times smaller than the sulfuric acid concentration, some 85% intensity decrease can be observed. Interestingly, the further addition of unlabelled chloride ions does not change markedly the observed intensity, indicating that the competition of the adsorption processes involves either a mixed adsorbate structure or different active spots. Although the chloride ion adsorption seems to be slow, one cannot draw any conclusion on the adsorption rate since there could be a significant mass transport effect due to the small chloride ion concentration.

3.1.2. Adsorption of labelled Cl^- ions

Although the cyclic voltammetric curves of polycrystalline platinum electrode in 0.1 mol dm^{-3} $HClO_4$ shows that the system reacts to the addition of the chloride ions (see Figure 6), no signal could be detected as a result of the chloride ion adsorption. Data in Section 3.1.1. also indicated that chloride ions adsorb on the Pt surface even if the solution concentration is very small. Nevertheless, this adsorption could not be followed by the radiation intensity due to the low specific activity of the chloride ions. Therefore, the adsorption kinetics of the chloride ions in the absence of another radiolabelled species undergoing a reversible adsorption process cannot be measured at the smooth Pt(poly) electrode. Although the investigation was performed up to 800 mV and for large adsorption times, no meaningful results could be obtained from the radiation intensity on the chloride adsorption.

3.2. Results on smooth Au(poly)

The adsorption of sulfate/bisulfate and chloride ions on Au(poly) electrode surface has been extensively studied by several methods in addition to the in-situ radiotracer techniques [20 and the references cited therein]; i. e. piezoelectric microbalance [26] and in-situ FTIR [21]. In this section, the most important results of some anion (HSO_4^-/SO_4^{2-}, Cl^-) adsorption on smooth polycrystalline gold electrode surface will be summarized. The advantages and limitations of the applicability of the original version of thin gap method will also be shown that, similarly to the results on Pt(poly).

3.2.1. Adsorption of SO_4^{2-}/HSO_4^-

The time dependence of sulfate/bisulfate adsorption on smooth gold electrode is shown by Figure 7.a at potential value E = 1200 mV. The fast adsorption process of HSO_4^-/SO_4^{2-} is clearly demonstrated in Figure 7.a. The saturation surface excess at the measured potential value is reached within a period of less than 10 seconds. The slow decrease of the surface excess at E = 1200 mV potential value is caused by the trace amount of some contaminant ions (e.g. Cl^-) present in the solution. The results of study of mobility of HSO_4^-/SO_4^{2-} ions are shown in Figure 7.b. As it can be seen, the adsorbed ions can be mobilized from the surface by a large amount of inactive sulfate/bisulfate. The comparison of the two graphs in Fig. 7 indicate that not only is the adsorption of the sulfate species fast on the sulfate-free electrode surface but the adsorption is reversible in the sense that a fast adsorption-desorption equilibrium process takes place. The decrease in the radiation intensity upon the addition of the unlabelled sulfuric acid corresponds to the concentration ratio of the unlabelled and labelled sulfate species, thus indicating equilibrium between the dissolved and adsorbed species.

Figure 8.a shows the cyclic voltammogram curve of polycrystalline gold taken in c = 0.1 mol dm^{-3} $HClO_4$ in the absence (solid line) and in the presence (dotted line) of labelled H_2SO_4. The voltammetric behaviour of the gold electrode has a good agreement with the literature data [16, 22, 23, 27, 28, 48,]. It demonstrates well that the $HClO_4$/Au(poly) system satisfies the purity requirements for electrosorption studies. The comparison of voltammograms recorded in the absence and in the presence of sulfuric acid reveals that HSO_4^-/SO_4^{2-} ions in the electrolyte cause the onset of the electrooxidation of the gold surface to shift towards more positive potential values by ca. 100 mV, which is indicative of the site-blocking by surface interacting anions. The onset of the sulfate/bisulfate adsorption is at E = 50 mV, and the coverage increases the maximum value at E = 1275 mV. In Figure 8.b at the adsorption maximum, the coverage is only $\Theta \sim 0.07$, which means that the adsorption layer is by far not compact.

3.2.2. Adsorption of Cl^-

Figure 9 shows the time dependence of chloride anion adsorption and desorption. The fast adsorption process of Cl^- is clearly demonstrated at Figure 9.a. The saturation surface excess at the measured potential value is reached within a period less than 10 seconds. The

stability of the signal during the chloride ion adsorption was significantly better than in the case of the sulfate/bisulfate adsorption on either Pt(poly) or Au(poly) electrodes. This fact indicates that the impurity effect was negligible here; hence, this underpins the former assumption on the competitive co-adsorption of Cl^- ions besides the sulfate/bisulfate adsorbates. When the labelled adsorbate is $^{36}Cl^-$, however, the competitive effect of the chemically identical species is proportional to its concentration ratio, and the impact of the unlabelled chloride impurity is thus negligible.

The desorption section of Figure 9.a shows that the release of the chloride ions from the surface as a result of the potential change is equally fast as their adsorption. Similar conclusion can be drawn from the mobility experiment (Fig. 9.b). The addition of the large excess of unlabelled hydrochloric acid at E = 1200 mV results in the decrease in signal intensity related to the adsorbed active chloride ions. The exchange of the labelled to unlabelled chloride adsorbates is nearly instantaneous. Therefore, it is shown that a dynamic equilibrium of the adsorbed and solute chloride ions prevails in this system, too.

Figure 10.a shows the cyclic voltammetric curve of polycrystalline gold taken in 0.1 mol dm^{-3} $HClO_4$ in the absence (solid line) and in the presence (dotted line) of labelled HCl (labelled with ^{36}Cl). The voltammetric behaviour of the gold electrode is in good agreement with literature data [16, 22, 27, 23, 28, 48,]. A comparison of the solid line to the dotted line in Figure 10.a reveals that the presence of Cl^- ions in the electrolyte causes the onset of the electrooxidation of the gold surface to shift towards more positive potential values by approximately 250 mV, which is indicative of the site-blocking by surface interacting anions. The surface excess of Cl^- ions on polycrystalline gold as a function of the electrode potential is shown in Figure 10.b. This function corresponds well, within the experimental error bar, to the results published in literature [28 and the references therein]. The surface excess of the chloride ions achieves the maximum around E = 1200 mV. While electrostatic effects would lead to an increase of the surface coverage at more positive potentials, the competing oxygen adsorption (gold surface oxidation) results to a fairly ill-defined decrease in the coverage. The measurement of the surface excess at potentials more positive than 1600 mV is not possible due to the dissolution of Au in the presence of chloride ions.

3.3. Results on platinum black

The investigation of sulfate/bisulfate and chloride adsorption phenomena on different metal electrodes (stainless steel [24], Cu [29], Rh [13]) and on noble metal electrodes [25 and

the further literature cited therein] by in-situ methods is a well-known process, but on platinized platinum electrodes it is a lesser investigated phenomenon. The latter was mostly dealt with by G. Horányi [30-32, 40,].

3.3.1. Adsorption of SO_4^{2-}/HSO_4^-

No previous results can be found for the investigation of sulfate/bisulfate adsorption on rough surfaces of platinum measured by in-situ thin gap radiotracer method.

The precision of the surface excess values determination of sulfate/bisulfate adsorption by using equation (2) is not satisfying on the porous platinum black surface. This can be explained by the small escape depth of the electron from the porous layer. The escape depth of the electron in aqueous solutions is lower than 300 μm, which is due to the low β_{max} – energy of ^{35}S radionuclide. This escape depth is further decreased by the radiation absorption of the porous Pt layer. The adsorption results of this section will be shown in radiation intensity values (I_{ads}) in order to illustrate the increased radiation adsorption capability of porous platinized platinum surface compared to the smooth platinum surface. The results of sulfate/bisulfate adsorption on platinized platinum are demonstrated on electrodeposited porous Pt layers with $k = 0.5$ μm thickness and $\gamma = 57$ surface roughness.

The time dependence of sulfate/bisulfate adsorption on rough platinum electrode is shown in Figure 11.a at potential value E = 750 mV. The slow accumulation process of HSO_4^-/SO_4^{2-} is clearly demonstrated at Figure 11.a. The saturation intensity value at the measured potential value is achieved within a period of more than 6 minutes. The slow increase of the saturation intensity values at E = 750 mV potential value compared to the fast adsorption process results on Pt(poly) can be explained by the significant difference in the roughness factors. Furthermore, it can be caused by two facts: (i) The accumulation of the active (labelled) anions requires a diffusion from much larger distance than in the case of smooth electrodes. This makes the adsorption process apparently slow; nevertheless, the rate-determining step is likely the mass transport and not the adsorption process itself when the anion reaches the platinum surface. (ii) The diffusion in the pores can be much hindered as compared to the bulk electrolyte solution, which apparently decelerates the adsorption.

The results of study of mobility of HSO_4^-/SO_4^{2-} ions are shown in Figure 11.b. As it can be seen, the labelled adsorbed ions on platinized platinum can be mobilized from the surface only partly by a large amount of inactive sulfate/bisulfate. The time constant of adsorption (Fig. 11.a, curve 2) and the adsorbate replacement (Fig. 11.b, curve 2) are

approximately the same. Since the intensity decrease due to the addition of a large excess of unlabelled sulfuric acid is not proportional to the concentration ratio of the labelled and unlabelled species, it can be concluded that a part of the adsorbate at the porous Pt surface is not mobile. It is reasonable that the porous Pt layer may exhibit a great variety of adsorption sites suitable for the sulfate/bisulfate anions, and hence, the adsorption at the sites of highest binding energy may also be irreversible at 750 mV. This can be caused by various factors. For instance, if the surface roughness of Pt is high also at the atomic level, the adsorbed anions can be surrounded with surface Pt atoms at a much larger extent than on smooth surfaces. Therefore, their mobility can be limited in porous layers of high roughness. Interestingly, the potential change to 50 mV leads to a fast a complete desorption process.

Voltammetric studies of the rough surface of platinized platinum electrode are shown by Figure 12.a. Here, the positive potential limit was E = 750 mV in order to prevent both the rearrangement of the surface atoms and the decrease in the surface roughness. Compared to the curve obtained for the sulfate-free electrolyte solution, it can be seen that in the presence of Na_2SO_4 the starting potential value of the more negative H-adsorption and desorption of the platinum black surface is shifted towards negative values, which is caused by the active-centre blocking effect of the adsorbed anions. It can be also established that in the potential region where the sulfate/bisulfate ions no longer adsorb on the Pt surface (i.e., for E < 150 mV), the sulfate/bisulfate ions do not affect the hydrogen adsorption curve.

The saturation intensity values of HSO_4^-/SO_4^{2-} ions on platinum black as a function of the electrode potential are shown in Figure 12.b. Compared the sulfate/bisulfate ion adsorption experiments to the result on smooth Pt(poly) electrodes, the enhanced active surface area of Pt black electrodes provides a significantly larger radiation signal intensity for the sulfate/bisulfate ion adsorption measrement. An approximately linear increase in the surface excess values was found as the electrode potential was increased up to E = 750 mV.

3.3.2. Adsorption of Cl^-

The investigation of the adsorption of Cl^- ions on porous surface measured by in-situ thin gap method obtained much less attention than the same process measured by in-situ foil method. The latter was investigated by several methods [31, 40].

Figure 13.a shows the time dependence of chloride anion adsorption on the porous surface of platinum black at deposited layer thickness k = 1 μm and roughness factor γ = 69. The saturation surface excess at the measured potential value is achieved within a period of

more than 10 minutes. Although the direct comparison to the chloride adsorption on Pt(poly) surface is not possible due to the low signal intensity on the latter electrode, it can be seen that the adsorption process on the rough Pt electrode is significantly slower than the adsorption of any anion on either Pt or Au surface if smooth metal surfaces are used. This can be explained by the facts described in Section *3.3.1* as well: (i) The accumulation of the active (labelled) anions requires a diffusion from much larger distance than in the case of smooth electrodes. This makes the adsorption process apparently slow; nevertheless, the rate determining step is likely the mass transport and not the adsorption process itself when the anion reaches the platinum surface. (ii) The diffusion in the pores can be much hindered as compared to the bulk electrolyte solution, which apparently decelerates the adsorption.

The study of the mobility of the Cl^- ions within the porous layer of 1 μm thickness (γ=69) strongly supports the importance of the mass transport in the surface saturation when only the labelled chloride ions were present in the solution in very small concentration. When a 100 times larges excess unlabelled chloride ion concentration is applied (see Fig. 13.b), the intensity of the radiation signal decreases quite abruptly. The relatively high chloride ions concentration decreases the accumulation time of the adsorbate significantly, and hence, the apparent rate constant of the radiation signal decay is characteristic of the adsorbate exchange process itself, not to the mass transport. This experiment clearly shows that a fast adsorbate exchange equilibrium holds also at the Pt black electrode, similarly to the Au(poly) surface.

However, it is also demonstrated in Figure 13.b at arrow 1 that the chloride adsorption is only partly reversible by the addition of $c = 2 \times 10^{-2}$ mol dm^{-3} inactive HCl. The loss of signal intensity is much smaller than what would be expected with the assumption of the complete reversibility. While the excess of the unlabelled chloride ions was 100 times as compared to the labelled species, a sixfold decrease in the radiation intensity could be measured. The intensity measured after a fast decay period (approximately 20 s) slowly decreases, indicating that adsorption sites of various bond strength (or with various desorption rate constant) should be taken into account. Nevertheless, whichever kind of adsorption sites are involved in the chloride ion accumulation on the Pt black surface, all chloride ions can be removed by the shift of the potential value to E = 50 mV. In this sense, the inproportional adsorbate exchange seems to be the general feature of the porous Pt electrode since it was observed for the sulfate/bisulfate adsorption, too.

Cyclic voltammetric curves of the rough surface of platinum black electrode (γ = 69) are shown by Figure 14.a. Here, the positive potential limit was E = 750 mV in order to

prevent both the rearrangement of the surface atoms and the decrease in surface roughness. The voltammograms obtained are in good agreement with literature data [16-18] for both the perchloric acid solution and the chloride-doped electrolyte. Compared to the curve obtained for the chloride-free electrolyte solution, it can be seen that in the presence of HCl the starting potential value of the more negative H-adsorption and desorption of the platinum black surface is shifted towards negative values, which is caused by the active-centre blocking effect of the adsorbed anions. It can be also established that in the potential region where the chloride ions no longer adsorb on the Pt surface (i.e., for $E < 150$ mV) the chloride ions do not affect the hydrogen adsorption curve.

The average surface excess values of Cl^- ions for 5 different thicknesses of platinized platinum (γ ranging from 12 to 69) as a function of the electrode potential are shown in Figure 14.b. The results shown in Fig.14.b. were calculated by using Eq.(2), which was evaluated for porous electrodes. Despite the chloride ion adsorption experiments on the smooth Pt(poly) electrode were totally inconclusive, the enhanced active surface area of the Pt black electrodes provides a large enough radiation signal intensity for the chloride ion adsorption measrement also on the Pt surface. An approximately linear increase in the surface excess was found as the electrode potential was increased up to $E = 750$ mV.

4. Conclusion

The thin gap radiotracer method allows us to measure the potential-dependent adsorption of labelled sulfate/bisulfate (having a high specific activity) in dilute aqueous solution ($c \leq 2\times10^{-4}$ mol dm^{-3}) on the oxide-free surface of platinum electrode ($\gamma < 2$). The adsorption of HSO_4^-/SO_4^{2-} ions on the electrode proved to be rapid and the saturation Γ value at any adsorption potential is achieved in a period of less than 10 seconds. The reproducibility of the measurable surface excess in ClO_4^- supporting electrolyte during the weak adsorption of the HSO_4^-/SO_4^{2-} ions is essentially influenced by the formation of the electrode surface (purity, roughness factor) and also by the competitive adsorption of trace amount of impurities (particularly Cl^- ions). The surface coverage of adsorbed sulfate ions is very small, it does not exceed 0.25 monolayer in the whole interval of the examined potential. A large excess of inactive sulfate compound added into the solution phase mobilizes the labelled sulfate ions adsorbed on the surface. However, the sulfate ions can be mobilized in the presence of large excess of boric acid ($c = 1\times10^{-2}$ mol dm^{-3}) only. The interaction of the

chloride ions with the surface is stronger than of bisulfate/sulfate ions. The presence of even a trace amount of chloride ion in the solution phase reduces significantly the surface concentration of sulfate ions.

It should be highlighted, however, that the adsorption of Cl^- ion (labelled with ^{36}Cl, having a low specific activity) on the surface of polycrystalline platinum electrodes with small roughness factors ($\gamma < 2$) under the previously discussed conditions cannot be measured with the original version of in-situ thin gap radiotracer method. It is only the mobilization of the adsorbed sulfate/bisulfate ions that allows us to conclude the chloride ion adsorption.

The sequence of the relative adsorption strength of the examined anions on polycrystalline platinum electrode surface is as follows:

$$ClO_4^- < H_2BO_3^- < HSO_4^-/SO_4^{2-} < Cl^- .$$

Similarly to the results of Pt(poly), it can be stated that the saturation Γ values on the polycrystalline gold surface at the potential value E = 1200 mV are achieved within a period of less than 10 seconds. The potential-dependent adsorption of the labelled Cl^- and SO_4^-/HSO_4^{2-} ions are measurable on the oxide-free smooth gold surface. The maximum value of the surface excess in case of sulfate/bisulfate ions at potential value E = 1200 mV is $\Gamma = 7\times10^{-11}$ mol cm^{-2}. A large excess of inactive chloride added into the solution phase mobilizes the labelled sulfate/bisulfate ions adsorbed on the surface instanteneously.

The data shown in Figure 11-13 indicate that the adsorption of Cl^- ion (labelled with ^{36}Cl) on the smooth surface of the polycrystalline gold electrode under the previously discussed conditions can be measured by the in-situ thin gap radiotracer method. Despite the low specific activity, the saturation Γ value is measurable at the potential value E = 1200 mV and the maximum surface excess does not exceed $\Gamma = 2\times10^{-9}$ mol cm^{-2} (Θ = 1.33 ML based on the nearest neighbour atomic distances [28]). The adsorption is fast, and the adsorbed labelled Cl^- ions can be mobilized by a large amount of unlabelled chloride anions.

The improved version of the thin gap radiotracer method allows us to measure the potential-dependent adsorption of labelled chloride ions (having low specific activity) in dilute aqueous solutions ($c \leq 2\times10^{-4}$ mol dm^{-3}) on the oxide-free surface of platinum black ($\gamma > 10$). Although the application of a Pt electrode with high surface roughness leads to an substantial increase in the radiation intensity related to the sulfate/bisulfate adsorption, the quantitative determination of the surface excess and surface coverage was not possible. While the adsorbed quantity of the sulfate/bisulfate ions increases proportionally with the roughness factor of the electrode, the self-absorption of the porous Pt layer is rather significant for the

low-energy emission of ^{35}S, as opposed to that of ^{36}Cl. Therefore, this method is not applicable to determine the surface excess quantitatively for labelled sulfate/bisulfate ions in a concentration of 2×10^{-4} mol dm^{-3}. Nevertheless, the adsorption-capability of the rough surface is clearly preferable than that of the smooth surface.

Numerous parameters can be in-situ examined with the further developed in-situ thin gap radiotracer method. In this way it can be concluded that the adsorption of Cl^- ions on the rough electrode surface – compared to the time dependence of smooth electrode surfaces – is slow and the saturation Γ value at the typical given potential is formed in the period more than 10 minutes. This phenomenon can be explained by the penetration of the labelled ions of the porous surface. The maximum value of the saturation Γ value at potential value E = 750 mV was given $\Gamma = 4\times10^{-10}$ mol cm^{-2}. The adsorbed labelled chloride ions can be mobilized partly by the addition of large amount ($c = 2\times10^{-2}$ mol dm^{-3}) of inactive HCl. After achieving the steady-state of the chloride ion adsorption on the rough Pt electrode, the adsorbed ions can be completely desorbed by shifting the potential value from E = 750 mV to E = 50 mV. In this respect, the behaviour of the smooth and porous Pt elecrodes is analogous.

Acknowledgement

This work was supported by the Paks NPP Co. Ltd. (Paks, Hungary) and the TAMOP 4.2.1.B-09/1/KONV 2010-0003 project.

References

[1] G. Hevesy, About the exchange of atoms between solid and liquid interfaces (in German), Phys. Zeitschrift XVI. (1915) 52.

[2] A. Vértes, George Hevesy (in Hungarian), Magyar Kém. Folyóirat, 107 (2001) 412.

[3] F. Joliot-Curie, Electrochemical Study of the Application of Various Radionuclides (in French), J. Chim. Phys. Phys.-Chim. Biol. 27 (1930) 119.

[4] G. Horányi, Radiotracer Studies of Adsorption/Sorption Phenomena at Electrode Surfaces in: A. Wieckowski (Ed.), Interfacial Electrochemistry, Marcel Dekker Inc., New York, 1999, p. 477.

[5] K. Varga, Application of Combinated Radiotracer and Electrochemical Methods for the Investigation of solid/liquid interfaces (in Hungarian), Kémiai Közlemények 83 (1996) 77.

[6] G. Aniansson, The Radioactive Measurement of the Adsorption of Dissolved Substances on Liquid Surfaces and an Application to "Impurities" in Dodecyl Sodium Sulfate Solutions, J. Phys. Chem. 55 (1951) 1286.

[7] A. Wieckowski, The Direct Radiometric Study of Electrosorption of Tritium Labeled Compounds. Adsorption of Methanol on Gold Electrodes, J. Electrochem. Soc. 122 (1975) 252.

[8] A. Wieckowski, J. Sobkowski, Comparative Study of Adsorption and Oxidation of Formic Acid and Methanol on Platinized Electrodes in Acidic Solution, J. Electroanal. Chem. 63 (1975) 365.

[9] S. Smolinski, J. Sobkowski, Influence of the silver electrode surface structure on electrochemical adsorption of thiourea in perchloric acid solution, Polish Journal of Chemistry 75 (2001) 1493.

[10] M.S. McGovern, P. Waszczuk, A. Wieckowski, Stability of carbon monoxide adsorbed on nanoparticle Pt and Pt/Ru electrodes in sulfuric acid media, Electrochim. Acta 51 (2006) 1194.

[11] L. M. Rice, E. K. Krauskopf, A . Wieckowski, Single Crystal Radio-Elecrochemistry: Adsorption of Aceti Acid on Well-Defined Pt (111) Surfaces, J. Electroanal. Chem. 239 (1988) 413.

[12] E. K. Krauskopf, K. Chan, A. Wieckowski, In Situ Radiochemical Characterization of Adsorbates at Smooth Electrode Surfaces, J. Phys. Chem. 91 (1987) 2327.

[13] G. Horányi, M. Wasberg, Comparative radiotracer study of the adsorption of Cl^-, HSO_4^- (SO_4^{2-}) and H_2PO_4 anions on rhodized electrodes, J. Electroanal. Chem. 404 (1996) 291.

[14] A. Kolics, G. Horanyi, Some considerations about the applicability of the in situ radiotracer „foil" method for the study of accumulation processes on compact stainless steel electrodes-I. Measurement of β-radiation, Electrochim. Acta 41 (1996) 791.

[15] A. Kolics, Instrumentation in: G. Horányi (Ed.), Radiotracer Studies of Interfaces, Interface Science and Technology, Vol. 3., Elsevier B.V., Amsterdam, 2004, p. 279.

[16] H. Argenstein-Kozlowska, Surfaces, Cells, and Solutions for Kinetics Studies, in: E.Yeager, J. O'M. Bockris, B. E. Conway, S. Sarangapani (Eds.), Comprehensive Treatise of Electrochemistry, Vol. 9., Plenum Press, New York and London, 1984, p. 15.

[17] R. Buják, K. Varga, In situ radiotracer and voltammetric study of the formation of surface adlayers in the course of Cr(VI) reduction on polycrystalline and (111) oriented platinum, Electrochim. Acta 52 (2006) 332.

[18] A. Kolics, A. Wieckowski, Adsorption of bisulfate and sulfate anions on Pt(111) electrode, J. Phys. Chem. B. 105 (2001) 2588.

[19] G. Horányi, Recent developments in the application of the radiotracer method to the investigation of adsorption and catalytic phenomena, Electrochim. Acta 25 (1980) 43.

[20] G. Horányi, E. M. Rizmayer, P. Joó, Radiotracer study of the adsorption of Cl^- and HSO_4^- ions on a porous gold electrode and on underpotential deposited metals on gold, J. Electroanal. Chem. 152 (1983) 211.

[21] M. Weber, F. C. Nart, New Results on the Adsorption of Sulfate Species at Polycrystalline Gold Electrodes. An in Situ FTIR Study, Langmuir 12 (1996) 1895.

[22] R. Marczona, K. Varga, Adsorption phenomena on polycrystalline gold electrode modified by Zn adatoms, J. Radioanal. Nucl. Chem. 269 (2006) 29.

[23] P. Zelenay, L. M. Rice-Jackson, A. Wieckowski, Radioactive labelling study of sulfate/bisulfate adsorption on smooth gold electrodes, J. Electroanal. Chem. 283 (1990) 389.

[24] K. Varga, P. Baradlai, A. Vértes, In-situ radiotracer studies of sorption processes in solutions containing (bi)sulfite ions-II. Low carbon steel Electrochim. Acta 42 (1997) 1157.

[25] J. O'M. Bockris, M. Gamboa-Aldeco, M. Szklarczyk, Ionic adsorption at the solid-solution interphase using three in-situ methods, J. Electroanal. Chem. 339 (1992) 355.

[26] X. C. Jiang, M. Seo, N. Sato, Piezoelectric Response to Specific Asorption of Chloride Ions on Gold Electrode, J. Electrochem. Soc. 137 (1990) 3804.

[27] K. Varga, I. Szalóki, L. Gáncs, R. Marczona, Novel application of an in situ radiotracer method for study of the formation of surface adlayers in the course of Cr(VI) reduction on a gold electrode, J. Electroanal. Chem. 524-525 (2002) 168.

[28] A. Kolics, A. E. Thomas, A. Wieckowski, ^{36}Cl labelling and electrochemical study of chloride adsorption on a gold electrode from perchlorid acid media, J. Chem. Soc., Faraday Trans. 92 (1996) 3727.

[29] G. Horányi, Radiotracer study of interactions of anions and adatoms on metal surfaces with high real surface area - Specific anion adsorption accompanying the equilibrium formation and dissolution of Cu and Bi adlayers on a platinized platinum electrode, ACH Models Chem 134 (1997) 33.

[30] G. Horányi, J. Solt, F. Nagy, Investigation of adsorption phenomena on platinized platinum electrodes by tracer methods, J. Electroanal. Chem. 31 (1971) 87.

[31] G. Horányi, E. M. Rizmayer, Radiotracer study of the sdsorption of Cl^- ions in the course of monolayer oxide film formation at platinized platinum electrodes, Electrochim. Acta 30 (1985) 923.

[32] G. Horányi, Influence of the specific adsorption of anions ont he „double layer region" of the cyclic voltammetric curves obtained with platinized platinum, Solid State Electrochem. 2 (1998) 237.

[33] V. E. Kazarinov, A New Electrochemical Method for the Study of Adsorption from Solutions (in Russian), Elektrokhimija 2 (1966) 1170.

[34] K. Varga, G. Hirschberg, P. Baradlai, M. Nagy, Combined Application of Radiochemical and Electrochemical Methods for the Investigation of Solid/Liquid Interfaces in: E. Matijevic (Ed.), Surface and Colloid Sci., Vol. 16, Kluwer Academic/Plenum, New York, 2001, p. 341.

[35] K. Varga, The role of interfacial phenomena in the contamination and decontamination of nuclear reactors, in: G. Horányi (Ed.), Radiotracer Studies of Interfaces, Interface Science and Technology, Vol. 3, Elsevier B.V., Amsterdam, 2004, p. 313.

[36] D. Horváth, K. Berkesi, K. Varga, L. Péter, T. Kovács, R. Buják, T. Pintér, Development and application of the in-situ radiotracer thin gap method for the investigation of corrosion processes I. Adaptation of the thin gap method for the application of porous surfaces, Electrochim. Acta 109 (2013) 468.

[37] K. Berkesi, D. Horváth, K. Varga, Z. Németh, T. Pintér, L. Péter, Development and application of the in-situ radiotracer thin gap method for the investigation of corrosion processes II. Validation of the thin gap method adapted for the application of porous surfaces, Electrochim. Acta 109 (2013) 790.

[38] K. Varga, A. Szabó, R. Buják, The formation of radioactive contamination, investigation methods and decontamination in Nuclear Power Plants. (in Hungarian), in: B. Csákvári (Ed.), A kémia újabb eredményei, Akadémiai Kiadó, Budapest, 2007, p. 129.

[39] G. Hirschberg, Z. Németh, K. Varga, A detailed study of the reliability of some crucial parameters used in the in-situ radiotracer studies, J. Electroanal. Chem. 456 (1998) 171.

[40] G. Horányi, A novel approach to platinized platinum electrodes: specific adsorption as a partition between the solution phase and the electrodeposited platinum black layer, J. Electroanal. Chem. 417 (1996) 185.

[41] J. P. Gustafsson, Visual MINTEQ (Version 3.0b); Department of Land and Water Resources Engineering, KTH Royal Institute of Technology, Stockholm, 2010.

[42] H. B. Ortiz-Oliveros, E. Ordoñez-Regil, S. M. Fernández-Valverde, Sorption of uranium(VI) onto strontium titanate in KNO_3 medium, Journal of Radioanalytical and Nuclear Chemistry 279 (2009) 601.

[43] P. A. Christensen, A. Hamnett, Examples of the application of electrochemical methods, First ed., Chapter 3., Techniques and Mechanisms in Electrochemistry, Blackie Academic & Professional, London, 1994, p. 228.

[44] D. T. Sawyer, J. L. Roberts Jr., Electrode materials and their electrochemical behaviour, Chapter III., Experimental electrochemistry for chemists, John Wiley & Sons, New York, 1974, p 60.
[45] S. Shibata, The Activation of Platinum Electrodes by preoxidation, Bull. Chem. Soc. Japan 36 (1963) 525.
[46] W. G. French, T. Kuwana, Lifetime of Activated Platinum Surface, J. Phys. Chem. 68 (1964) 1279.
[47] H. Dietz, H. Göhr, About the electrochemical structure of oxygen and hydrogen-coverage on platinum in aqueous solution (in German), Electrochim. Acta 8 (1963) 343.
[48] M. Nagy, P. Baradlai, L. Tomcsányi, K. Varga, In situ radiotracer and voltammetric study of the mechanism of corrosion processes and the effects of corrosion inhibitors, Acta Chim. Hung. 132 (1995) 561.

Figures and figure caption

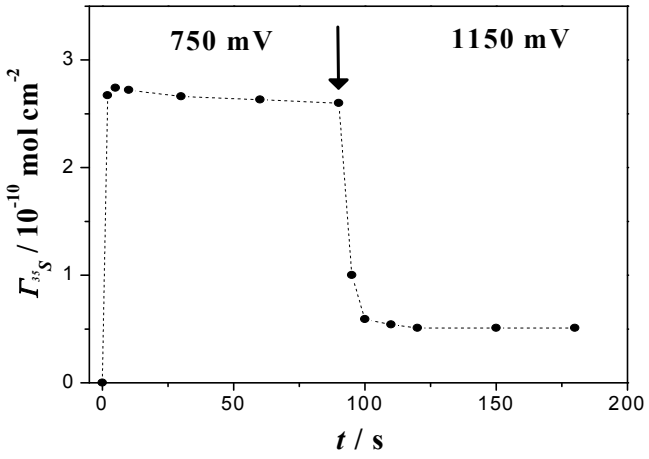

Figure 1

Time dependence of SO_4^{2-}/HSO_4^- (labelled with ^{35}S) adsorption on Pt(poly) in c = 0.1 mol dm^{-3} $HClO_4$ at the potential values of E = 750 mV and E = 1150 mV (the initial potential value at $t < 0$ was E = 50 mV). The shift of the potential value is indicated by an arrow.

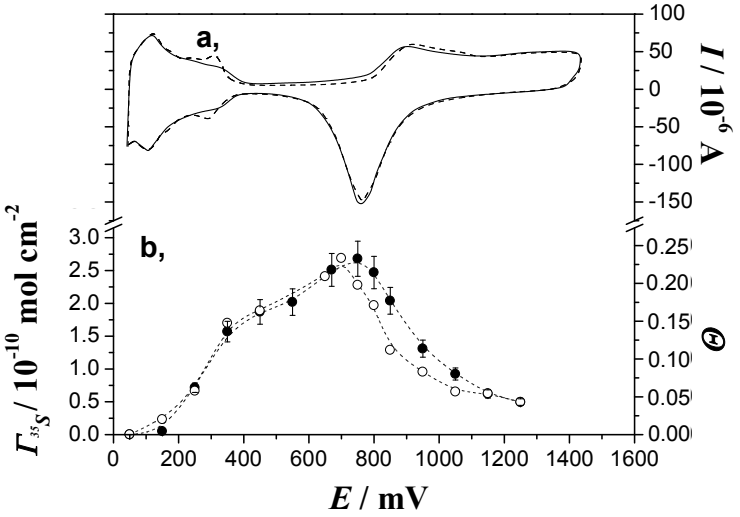

Figure 2

(a) Cyclic voltammetric curves recorded for Pt(poly) surface in c = 0.1 mol dm^{-3} $HClO_4$ in the absence (solid line) and presence (dotted line) of $c = 2 \times 10^{-4}$ mol dm^{-3} H_2SO_4 (labelled with ^{35}S). Sweep rate: 25 mV s^{-1}.

(b) Potential dependence of SO_4^{2-}/HSO_4^- adsorption on polycrystalline platinum electrode in the interrupted polarization mode. Curves 1 and 2 refer to the positive- and negative-going potential steps, respectively. The uncertainty of the Γ values determined by means of the error propagation relationship is indicated by error bars.

The monolayer coverage of SO_4^{2-}/HSO_4^- on the surfaces corresponds to $\Gamma = 1.15 \times 10^{-9}$ mol cm^{-2} (assuming the close fit of SO_4^{2-}/HSO_4^- anions [25]).

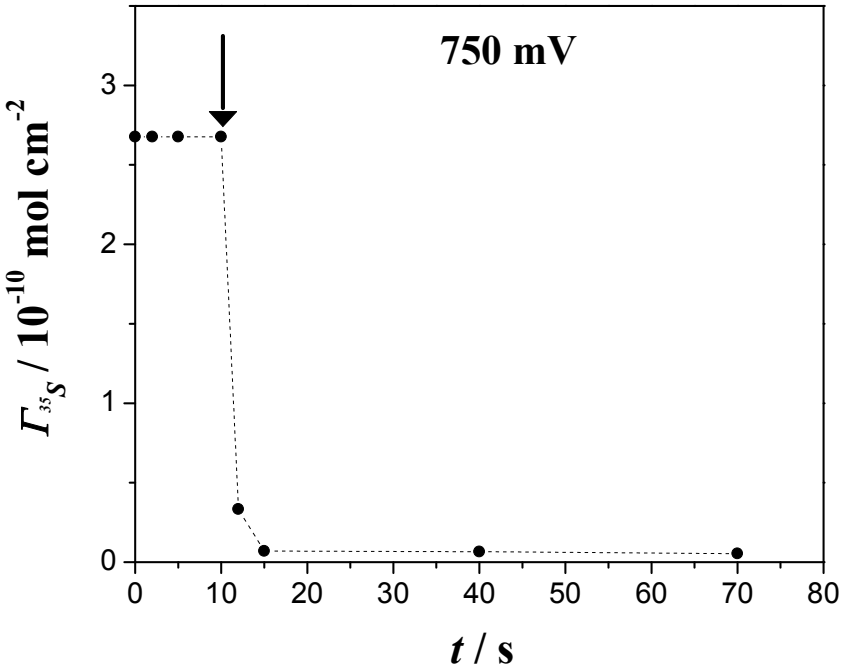

Figure 3

Study of the mobility of the adsorbed SO_4^{2-}/HSO_4^- species on Pt(poly) by the addition of $c = 2 \times 10^{-2}$ mol dm^{-3} unlabelled H_2SO_4. The moment of the addition is indicated by an arrow.

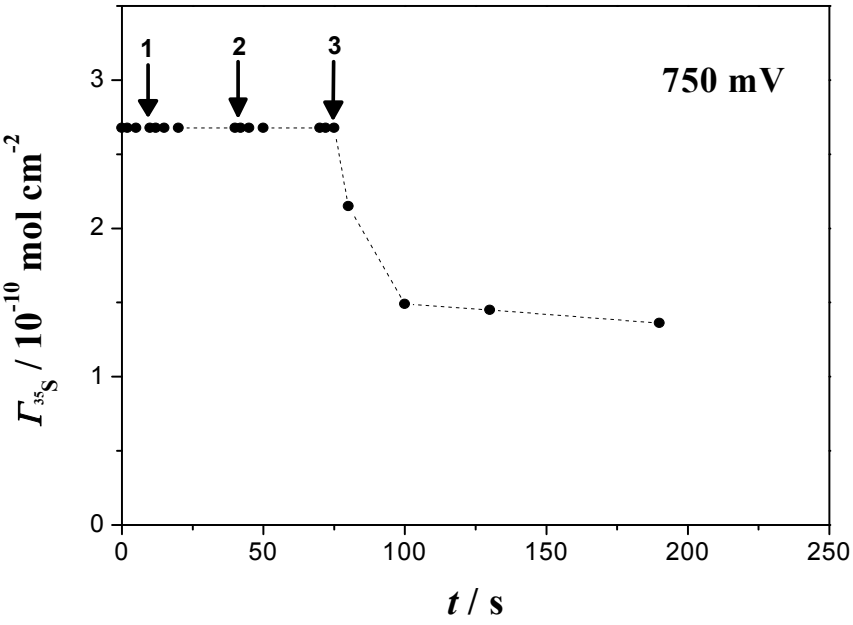

Figure 4

Study of the mobility of the adsorbed SO_4^{2-}/HSO_4^- species (labelled with ^{35}S) on Pt(poly) by the addition of (1) $c = 1 \times 10^{-4}$ mol dm^{-3}, (2) $c = 1 \times 10^{-3}$ mol dm^{-3}, (3) $c = 1 \times 10^{-2}$ mol dm^{-3} unlabelled H_3BO_3

The moments of the addition are indicated by arrows.

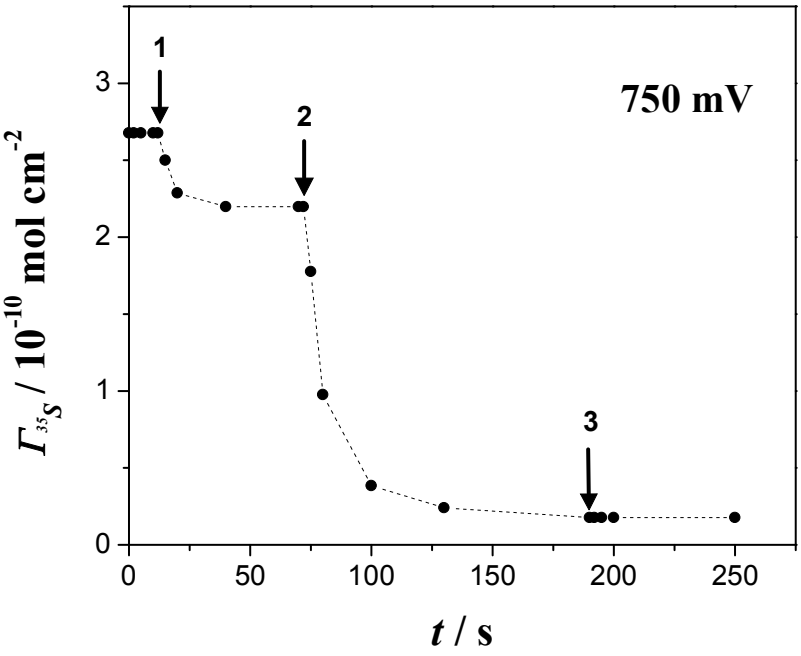

Figure 5

Study of the mobility of the adsorbed SO_4^{2-}/HSO_4^- species on Pt(poly) by the addition of (1) $c = 1 \times 10^{-6}$ mol dm^{-3}, (2) $c = 1 \times 10^{-5}$ mol dm^{-3}, (3) $c = 1 \times 10^{-4}$ mol dm^{-3} unlabelled HCl

The moments of the addition are indicated by arrows.

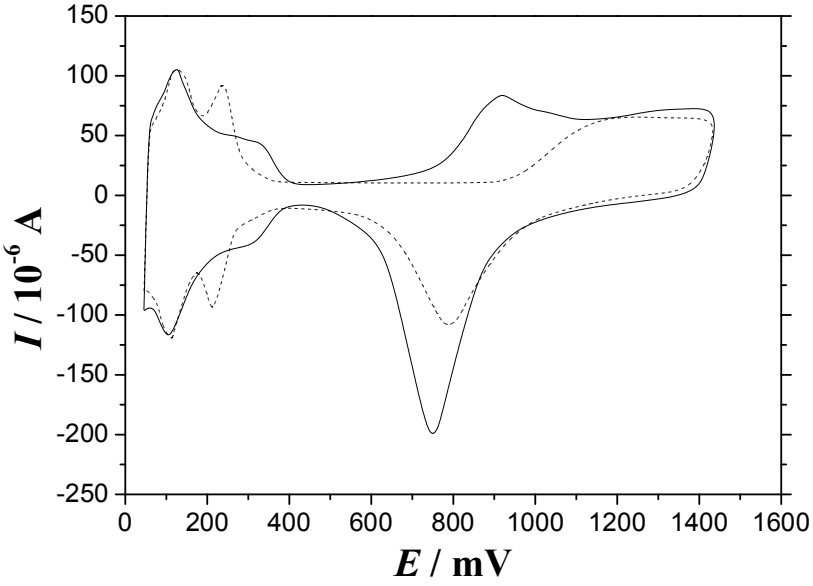

Figure 6

Cyclic voltammetric curves for a Pt(poly) electrode in $c = 0.1$ mol dm^{-3} $HClO_4$ in the absence (solid line) and presence (dotted line) of $c = 2 \times 10^{-4}$ mol dm^{-3} HCl (labelled with ^{36}Cl). Sweep rate: 100 mV s^{-1}.

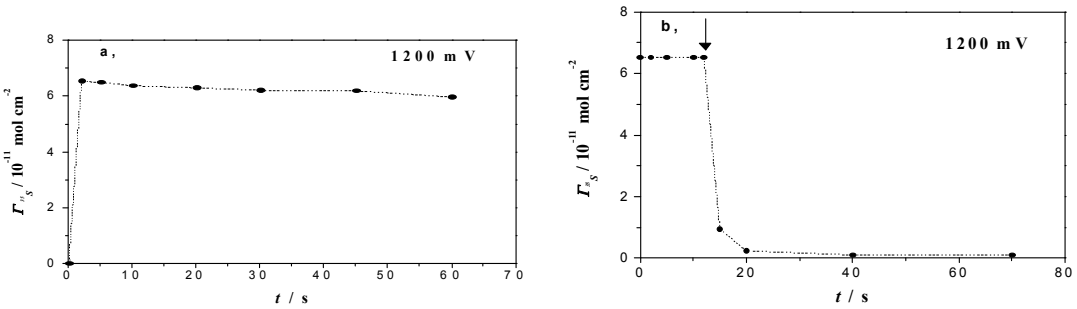

Figure 7

(a) Time dependence of SO_4^{2-}/HSO_4^- (labelled with ^{35}S) adsorption on Au(poly) in c = 0.1 mol dm^{-3} $HClO_4$ at the potential value of E = 1200 mV

(b) Study of the mobility of the adsorbed labelled SO_4^{2-}/HSO_4^- species on Au(poly) by the addition of $c = 2 \times 10^{-2}$ mol dm^{-3} unlabelled H_2SO_4

The moment of the addition is indicated by arrow.

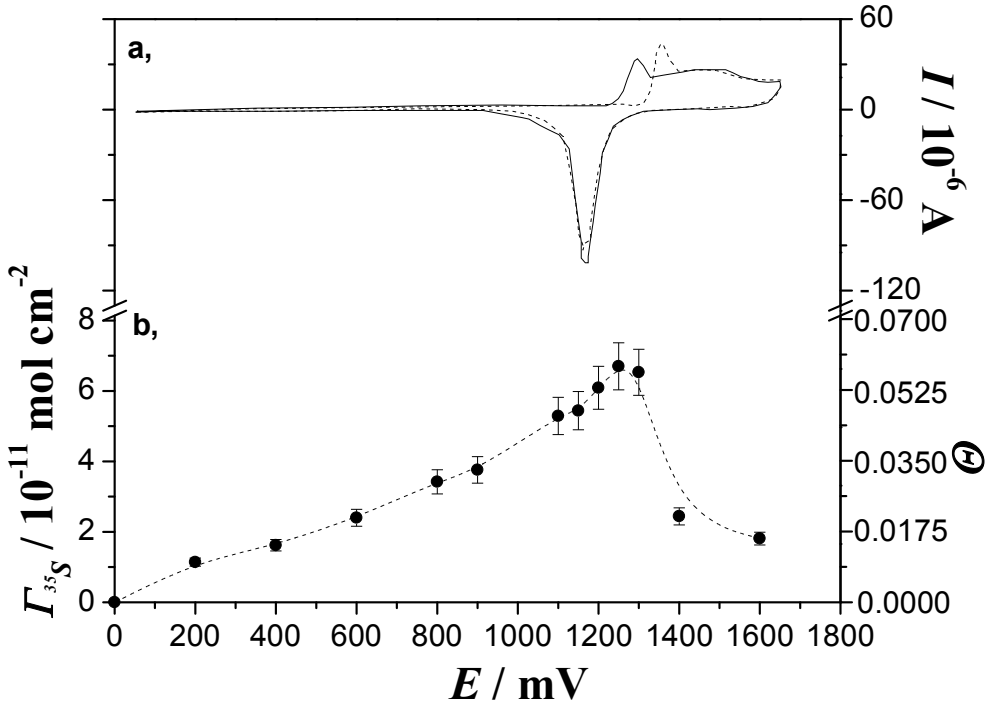

Figure 8

(a) Cyclic voltammetric curves at Au(poly) surface in c = 0.1 mol dm^{-3} $HClO_4$ in the absence (solid line) and presence (dotted line) of $c = 2 \times 10^{-4}$ mol dm^{-3} H_2SO_4 (labelled with ^{35}S). Sweep rate: 25 mV s^{-1}.

(b) Potential dependence of SO_4^{2-}/HSO_4^- (labelled with ^{35}S) adsorption on polycrystalline gold electrode in the interrupted polarization mode. The uncertainty of the Γ values determined by means of the error propagation relationship is indicated by error bars.

The monolayer coverage of SO_4^{2-}/HSO_4^- on the surfaces corresponds to $\Gamma = 1.15 \times 10^{-9}$ mol cm^{-2} (assuming the close fit of SO_4^{2-}/HSO_4^- anions [25]).

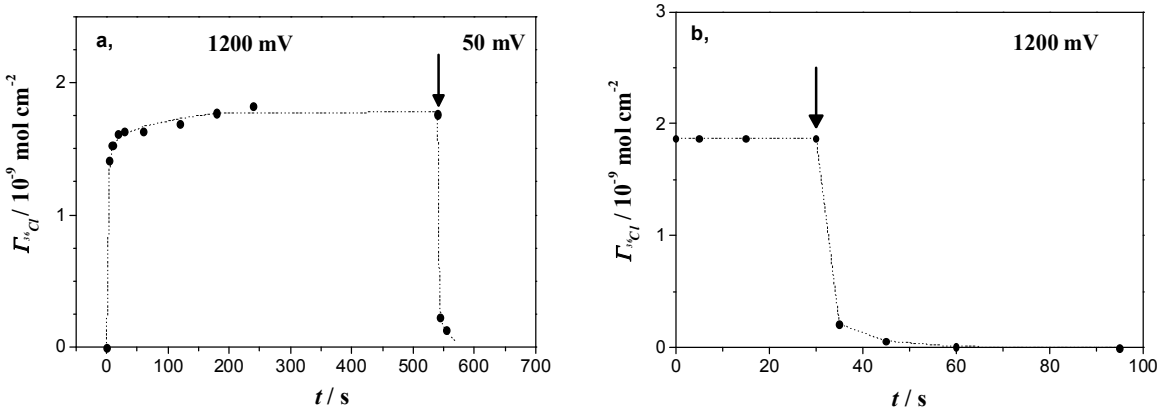

Figure 9

(a) Time dependence of Cl^- (labelled with ^{36}Cl) adsorption on Au(poly) in c = 0.1 mol dm^{-3} $HClO_4$ at the potential values of E = 1200 mV.
At the time indicated by the arrow, the potential value was changed to E = 50 mV.
(b) Study of the mobility of the adsorbed Cl^- species on Au(poly) by the addition of c = 2×10^{-2} mol dm^{-3} unlabelled HCl.
The moment of the addition is indicated by the arrow.

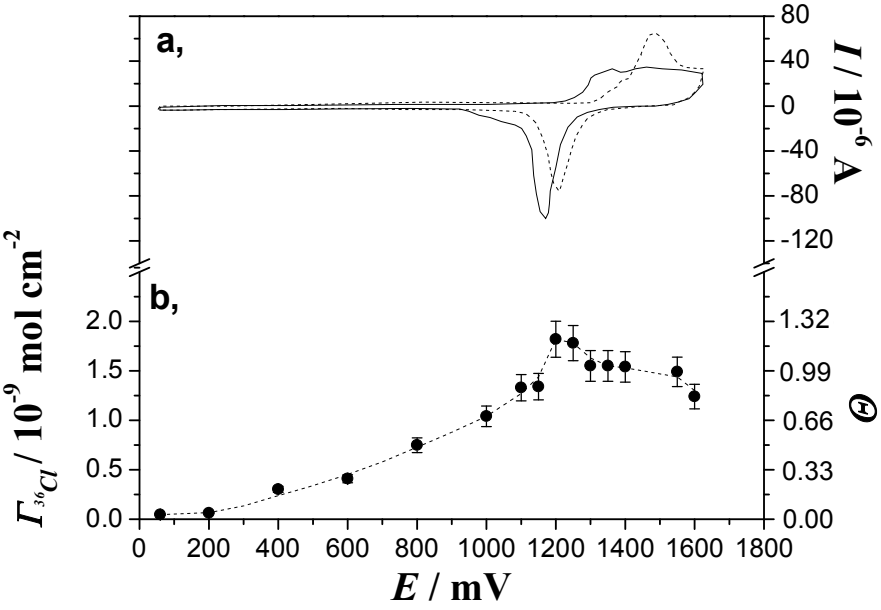

Figure 10

(a) Cyclic voltammetric curves at Au(poly) surface in c = 0.1 mol dm^{-3} $HClO_4$ in the absence (solid line) and presence (dotted line) of c = 2×10^{-4} mol dm^{-3} HCl (labelled with ^{36}Cl). Sweep rate: 25 mV s^{-1}.
(b) Potential dependence of Cl^- (labelled with ^{36}Cl) adsorption on polycrystalline gold electrode in the interrupted polarization mode. The uncertainty of the Γ values determined by means of the error propagation relationship is indicated by error bars.
The monolayer coverage of Cl^- on the surfaces corresponds to Γ = 1.5×10^{-9} mol cm^{-2} (for a close-packed hexagonal monolayer of Cl atoms assuming a 1.81 Å radius [28].

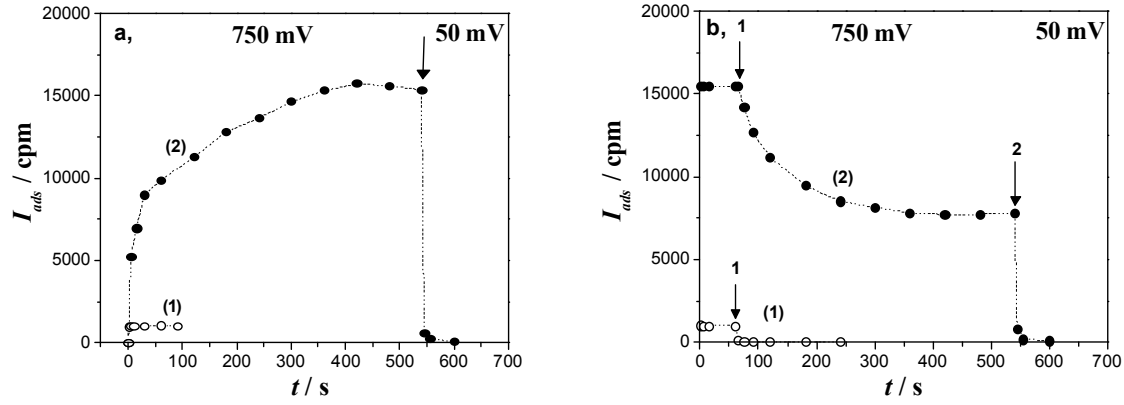

Figure 11

(a) Time dependence of SO_4^{2-}/HSO_4^- (labelled with ^{35}S) adsorption on smooth ($\gamma < 2$; curve 1) and rough ($\gamma = 57$; curve 2) surface of platinum in $c = 0.1$ mol dm^{-3} $HClO_4$ at the potential values of $E = 750$ mV.
At the arrow, the potential value was changed to $E = 50$ mV.
(b) Study of the mobility of the adsorbed SO_4^{2-}/HSO_4^- species on smooth platinum (1) and on platinum black ($\gamma = 57$) (2) by the addition of $c = 2 \times 10^{-2}$ mol dm^{-3} unlabelled Na_2SO_4.
The moment of the addition is indicated by Arrow 1.
The shift of the potential value to $E = 50$ mV is indicated by Arrow 2.

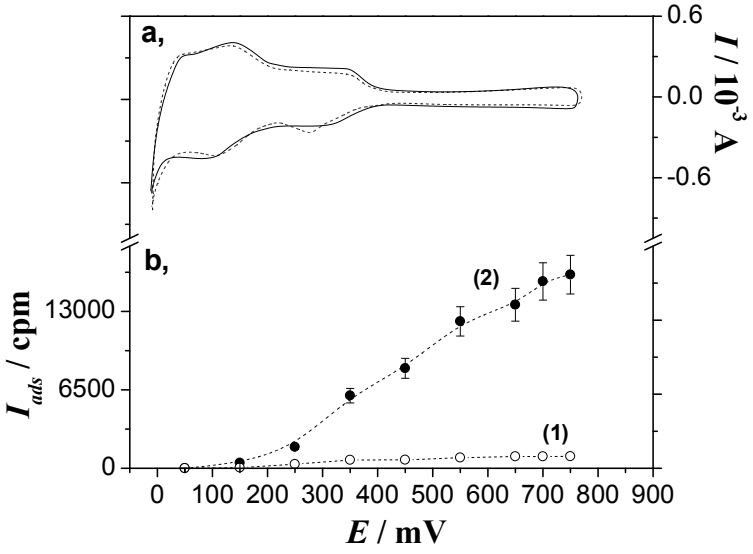

Figure 12

(a) Cyclic voltammetric curves at rough surface of platinum black ($\gamma = 57$) in $c = 0.1$ mol dm^{-3} $HClO_4$ in the absence (solid line) and presence (dotted line) of $c = 2 \times 10^{-4}$ mol dm^{-3} Na_2SO_4 (labelled with ^{35}S). Sweep rate: 25 mV s^{-1}.
(b) Potential dependence of SO_4^{2-}/HSO_4^- (labelled with ^{35}S) adsorption on Pt(poly) (1) and on platinized platinum (2) electrodes in the continuous polarization mode. The uncertainty of the I_{ads} values determined by means of the error propagation relationship is indicated by error bars.

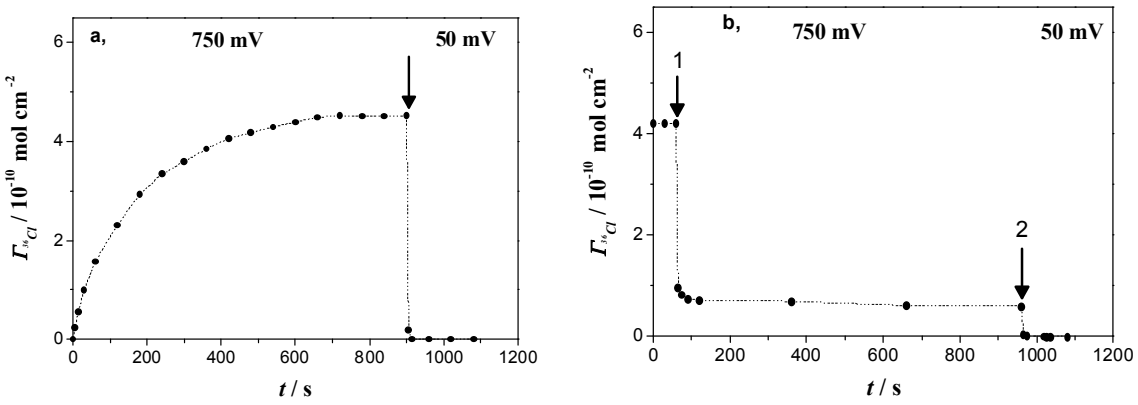

Figure 13

(a) Time dependence of Cl^- (labelled with ^{36}Cl) adsorption on rough surface of platinum black ($\gamma = 69$) in $c = 0.1$ mol dm^{-3} $HClO_4$ at the potential values of $E = 750$ mV
At the arrow, the potential value was changed to $E = 50$ mV.
(b) Study of the mobility of the adsorbed Cl^- species on platinum black ($\gamma = 69$) by the addition of $c = 2 \times 10^{-2}$ mol dm^{-3} unlabelled HCl.
The moment of the addition is indicated by Arrow 1.
The shift of the potential value to $E = 50$ mV is indicated by Arrow 2.

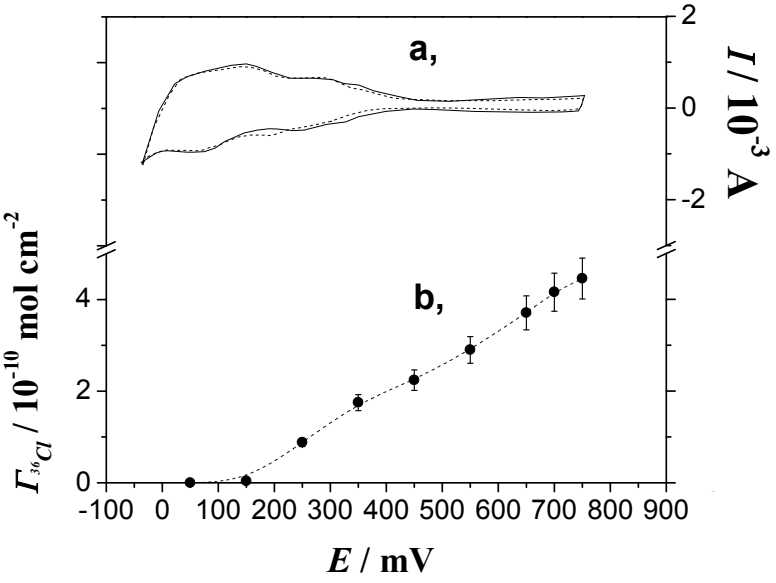

Figure 14

(a) Cyclic voltammetric curves at rough surface of platinum black ($\gamma = 69$) in $c = 0.1$ mol dm^{-3} $HClO_4$ in the absence (solid line) and presence (dotted line) of $c = 2 \times 10^{-4}$ mol dm^{-3} HCl (labelled with ^{36}Cl). Sweep rate: 25 mV s^{-1}.
(b) Potential dependence of Cl^- (labelled with ^{36}Cl) adsorption on platinized platinum electrodes (*roughness factors* are between 12 and 69) in the continous polarization mode. The uncertainty of the Γ values determined by means of the error propagation relationship is indicated by error bars.